Title

Carboxylated Fullerene at the Oil/Water Interface

Journal

ACS Applied Materials & Interfaces, 9(39)

ISSN

1944-8244

Authors

Li, Rongqiang

Chai, Yu

Jiang, Yufeng

et al.

Publication Date

2017-10-04

DOI

10.1021/acsami.7b07154

Peer reviewed

ACS APPLIED MATERIALS & INTERFACES

Research Article

www.acsami.org

Carboxylated Fullerene at the Oil/Water Interface

Rongqiang Li,[†,‡] Yu Chai,[‡,§] Yufeng Jiang,[‡,∥] Paul D. Ashby,[⊥] Anju Toor,[‡] and Thomas P. Russell[*,‡,#,▽]

[†]College of Chemistry and Pharmaceutical Engineering, Huanghuai University, Zhumadian, Henan 463000, P. R. China

[‡]Materials Science Division, Lawrence Berkeley National Laboratory, Berkeley, California 94720, United States

[§]Department of Materials Science and Engineering, University of California, Berkeley, California 94720, United States

[∥]Department of Applied Science and Technology, University of California, Berkeley, California 94720, United States

[⊥]Molecular Foundry Division, Lawrence Berkeley National Laboratory, Berkeley, California 94720, United States

[#]Polymer Science and Engineering Department, University of Massachusetts, Amherst, Massachusetts 01003, United States

[▽]Beijing Advanced Innovation Center for Soft Matter Science and Engineering, Beijing University of Chemical Technology, Beijing 100029, P. R. China

Supporting Information

ABSTRACT: The self-assembly of carboxylated fullerene with poly(styrene-*b*-2-vinylpyridine) (PS-*b*-P2VP) with different molecular weights, poly-2-vinylpyridine, and amine-terminated polystyrene, at the interface between toluene and water was investigated. For all values of the pH, the functionalized fullerene interacted with the polymers at the water/toluene interface, forming a nanoparticle network, reducing the interfacial tension. At pH values of 4.84 and 7.8, robust, elastic films were formed at the interface, such that hollow tubules could be formed *in situ* when an aqueous solution of the functionalized fullerene was jetted into a toluene solution of PS-*b*-P2VP at a pH of 4.84. With variation of the pH, the mechanical properties of the fullerene/polymer assemblies can be varied by tuning the strength of the interactions between the functionalized fullerenes and the PS-*b*-P2VP.

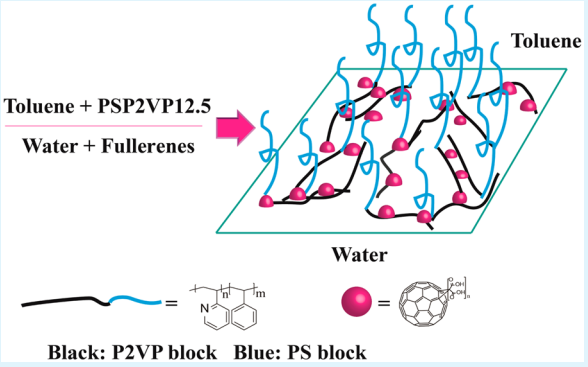

KEYWORDS: *assembly, interface, fullerene, nanoparticle surfactant, interaction*

1. INTRODUCTION

Colloids and nanoparticles, NPs, will assemble at fluid/fluid interfaces to lower the interfacial energy, forming emulsions that have attracted much theoretical and experimental attention[1−6] and have found use in the pharmaceutics, cosmetic, and food industries. NP assemblies at interfaces can be achieved by adsorption/desorption equilibrium or by interfacial interactions between functional NPs dispersed in one fluid and ligands with complementary functionality dissolved in a second fluid. Electrostatic interactions between NPs and ligands at the water/oil interface result in nanoparticle surfactants, which have been intensively investigated recently,[7−11] since the assembly of the NP surfactants at the interface can jam to lock in nonequilibrium shapes of liquids and are responsive to external stimuli. Most of the NPs in these previous studies have been polymeric or inorganic NPs. Regardless of the nature of the NPs, be they soft (polymeric) or hard (silica, Au, CdSe, etc.), the wettability of NPs by the fluids has been a critical factor in their self-assembly.[12−15]

The assembly of carbon-based nanomaterials at liquid/liquid interfaces has also been studied. Nanorods,[16] rod-like-virus particles,[17] and carbon nanotubes (single- or multi-walled) have been shown to assemble at liquid/liquid interfaces, assuming different orientations depending on the specific interfacial interactions and the areal density of nanorods at the interface.[18,19] Two-dimensional carbon materials, like graphene or graphene oxide, have also been found to be interfacially active, since each particle occupies a significant area at the interface.[20−23] As a zero-dimensional nanomaterial, fullerenes and their derivatives, though, have only received scant attention, even though they have very well-defined size, can be easily functionalized,[24] and are used in applications that draw on their electronic characteristics. The assembly of fullerene at liquid/liquid interfaces opens a new platform for fullerene-device applications.

Fullerene C60 is a 0.7 nm diameter polyhedral sphere. For an expansion in the potential use of this unique material, derivatives such as carboxylated, aminated, and polymer-grafted fullerenes have been developed.[25−27] The self-assembly of fullerene and its derivatives in solution and at interfaces has

Received: May 21, 2017
Accepted: September 8, 2017
Published: September 8, 2017

DOI: 10.1021/acsami.7b07154
ACS Appl. Mater. Interfaces 2017, 9, 34389−34395

been investigated.[28,29] While carboxylic-acid-functionalized fullerenes can be used for solution-based assembly processes,[30] their assembly at liquid/liquid interfaces, in particular at the oil/water interface, is of interest here. We consider the interactions between maleic-acid-functionalized fullerenes dispersed in water with polymers and block copolymers having complementary functionality, dissolved in oil, like toluene. With a variation in the number of complementary functional groups on polymers from mono-end-functionality to multifunctional homopolymers to multifunctional block copolymer, different properties of the interfacial assemblies have been achieved. Studies were performed as a function of the pH of the aqueous phase, which was found to dramatically alter the interfacial interactions. Plateau−Rayleigh instabilities of a jetted aqueous solution of the carboxylated fullerenes in a toluene solution of the block copolymers were suppressed, allowing the formation of aqueous tubules in toluene that could continuously transport the aqueous phase from one reservoir to another.

2. EXPERIMENT

2.1. Materials. Fullerene-*n*-maleic acid, where *n* denotes the number of maleic acid moieties attached to the fullerene and is typically on the order of 30−50, was purchased from Solaris Chem., Inc. Monoamine-terminated polystyrene ($PSNH_2$), poly(2-vinylpyridine) (P2VP), and poly(styrene-*b*-2-vinylpyridine) (PS-*b*-P2VP) diblock copolymers of different molecular weights and volume fractions of PS were purchased from Polymer Source and used without further purification. The different polymers used are shown in Table 1. Anhydrous toluene from Sigma-Aldrich was used as received.

Table 1. Molecular Weight and PDI of All Polymer Samples Used

material	M_n (g/mol)	PDI	abbreviation
poly(styrene-*b*-2-vinylpyridine)	7.5K-*b*-12.5K	1.05	PSP2VP12.5
poly(styrene-*b*-2-vinylpyridine)	16.5K-*b*-3.5K	1.05	PSP2VP3.5
poly(styrene-*b*-2-vinylpyridine)	23.6K-*b*-10.4K	1.04	PSP2VP10.4
monoamine-terminated polystyrene	2.5K	1.17	$PSNH_2$
poly-2-vinylpyridine	3.5K	1.16	P2VP

2.2. Characterization. The interfacial tension between the aqueous phase and toluene, the organic phase, was measured with a dynamic pendant drop tensiometer (Kruss GmbH Germany DSA30S). The volume of the droplets was controlled to be 15 μL. Interfacial dilatational rheology was performed using a pendant drop tensiometer coupled to an oscillation drop generator housing a piezoelectric element able to produce changes in drop surface area over broad ranges. In oscillatory experiments, fullerene-*n*-maleic acid containing a water drop was created inside a toluene solution of PS-*b*-P2VP (M_n = 16K-*b*-3.5K g/mol), and before the start of testing, with the drop volume fixed, interfacial assembly was allowed to reach steady-state. Analysis of a video recording of the drop shape provided γ as a function of time, which, in conjunction with area change, allowed calculation of the elastic modulus and loss modulus. The pH of the aqueous solution was measured with a Mettler Toledo EL-20 pH/conductivity meter. Atomic force microscopy (AFM) images were performed using a Digital Instruments Dimension 3100 AFM instrument. Plateau−Rayleigh instability experiments were carried using a syringe with a continuous pump and a high-frame-rate video camera. Different flow rates of fullerene solutions were jetted through a capillary with a 0.25 mm inner diameter into a toluene solution of polymer.

3. RESULTS AND DISCUSSIONS

3.1. Interfacial Tension of Carboxylate Fullerene at the Water/Toluene Interface. Solutions of the maleic-acid-functionalized fullerenes were prepared in water. Three different bulk solutions were used: one was a 1 g/L dispersion at a pH of 11.17; the second was 0.224 g/L at a pH of 7.8; and the third was a 0.08 g/L dispersion at a pH of 4.84. The interfacial tension between water and toluene was unchanged with the addition of maleic-acid-functionalized fullerene dispersed in the water. Consequently, the maleic-acid-functionalized fullerene is not interfacially active, since the water/toluene interface carries an inherent negative charge.[31] With P2VP dissolved in toluene, the interfacial tension of a water droplet (pH of 7.8, not containing the functionalized fullerene) was found to decrease. Similarly, if PS-*b*-P2VP (0.05 g/L) was dissolved in the toluene, the interfacial tension was found to decrease. In addition, the interface tension decreased with increasing concentration of PS-*b*-P2VP. This indicates that there was some quaternization of the 2VP, making the block polar and, hence, enhancing its interfacial activity. These results also indicate that the P2VP chains are adsorbing at the interface, placing multiple 2VP units at the interface; i.e., the P2VP chains are orienting preferentially parallel to the interface to increase the number of 2VP contacts with the water phase. The PS portion of the copolymer is, of course, solubilized in the toluene phase, since toluene is a good solvent for PS. If the maleic-acid-functionalized fullerenes are dispersed in the aqueous phase and the P2VP or PS-*b*-P2VP is dissolved in the toluene phase, an even greater reduction in the interfacial

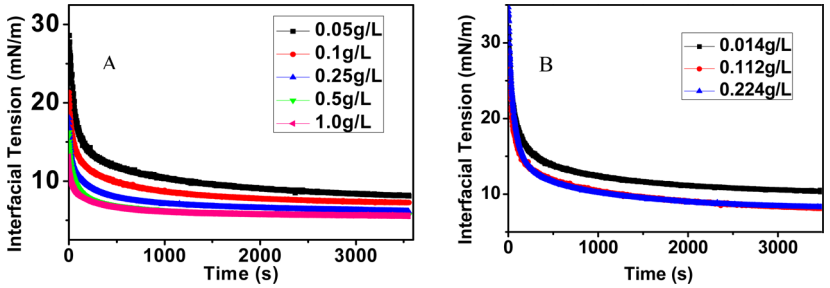

Figure 1. (A) Dynamic interfacial tension of 0.112 g/L fullerene aqueous solution at pH 7.8 in contact with a toluene solution of PSP2VP3.5 at different concentrations of the copolymer. (B) Dynamic interfacial tension for a fixed concentration of PSP2VP3.5 with an increasing concentration of the maleic-acid-functionalized fullerene at pH 7.8.

DOI: 10.1021/acsami.7b07154
ACS Appl. Mater. Interfaces 2017, 9, 34389−34395

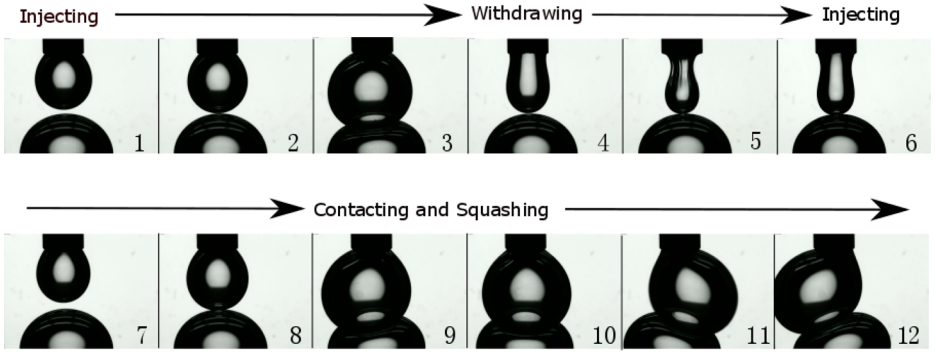

Figure 2. Sequence of snapshots during the pendant drop experiment, where both the top and bottom droplets were formed by injecting 0.224 g/L carboxylated fullerene aqueous solution into 0.05 g/L PSP2VP3.5 toluene solution. The bottom droplet was formed prior to the experiment and pinched at the bottom of the cuvette. Images 1−3 and 6−8 show the expansion of the top droplet by continuously injecting carboxylated fullerene aqueous solution, while images 4 and 5 depict the withdrawing process. The last four images describe the swinging motion between the two droplets, which was realized by controlling the relative location between the needle and cuvette. The size of every image is 7.2 mm × 4.9 mm.

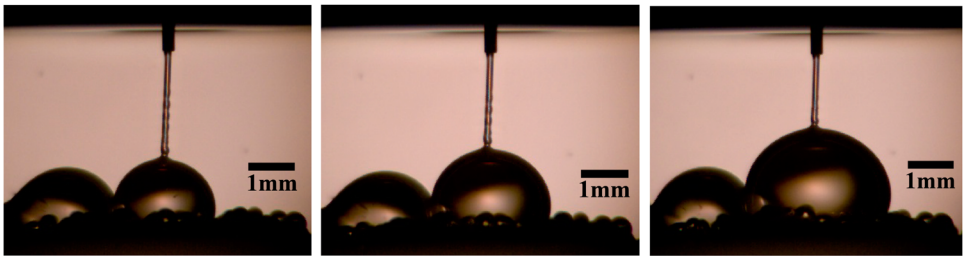

Figure 3. Imaging of continuous injection of 0.08 g/L carboxylated fullerene (pH = 4.84) aqueous solution (from the top needle) at the speed of 4 mL/min into the droplet (bottom) at the atmosphere of 0.1 g/L PSP2VP12.5K toluene solution through the tubule. The droplet volume increased with time.

tension is observed. Shown in Figures 1A are the interfacial tensions at a constant concentration of the maleic-acid-functionalized fullerene (0.112 g/L) in the water phase at a pH of 7.8 as a function of concentration of the copolymer for PSP2VP3.5. Similar plots for PSP2VP10.5 and PSP2VP12.5 (increasing P2VP molecular weight) are shown in Figure S1A,B. As can be seen, with an increase in concentration of the polymer, the interfacial tension in each system is decreased. Increasing the molecular weight of the P2VP caused a decrease in the interfacial tension, and similarly, for a fixed molecular weight, increasing the concentration of the P2VP causes the interfacial tension to decrease. Shown in Figure 1B is the interfacial tension for a fixed concentration (0.05 g/L) of PSP2VP3.5 with an increasing concentration of the maleic-acid-functionalized fullerene. Here, with increasing concentration of the fullerene, the interfacial tension is seen to decrease. From these combined results the picture that emerges is that the P2VP chains adsorb at the interface with multiple P2VP units in contact with the interface. With increasing molecular weight, the number of P2VP units at the interface increases. The adsorption of these chains at the interface occurs initially, since the maleic-acid-functionalized fullerenes are not interfacially active. After the P2VP chains adsorb, the maleic-acid-functionalized fullerenes diffuse to the interface and interact with the P2VP unit at the interface. Since there are ∼30 maleic acid units per fullerene, it is likely that the fullerenes interact with multiple chains, forming a cross-linked network at the interface that can extend into the aqueous phase.

The interactions between the maleic-acid-functionalized fullerenes and the P2VP and PS-*b*-P2VP are essentially acid−base type interactions, and as such, the pH of the aqueous phase will affect the dissociation of the acid and the protonation of the amine in the P2VP. Regardless of the pH, the maleic-acid-functionalized fullerene dispersed in water was not interfacially active, and the interfacial tension was essentially the same as that of water/toluene. Figure S2 shows the interfacial tension of a water droplet in a toluene solution of P2VP homopolymer as a function of time for different values of the pH, while Figure S3A,B,C shows the interfacial tension of a water droplet in a toluene solution of PS-*b*-P2VP copolymer as a function of time for different values of the pH, where the molecular weight of the P2VP block is 3.5K, 10.4K, and 12.5K g/mol. In all cases, the interfacial tension is markedly reduced, reflecting the surfactant-like nature of the block copolymer and the hydrophilic character of the P2VP block. While the rate at which the interfacial tension decreased depended on the molecular weight of the P2VP block, the polymer solution in the different pH condition without fullerene in water reached essentially the same interfacial tension at long times. At a pH of 7.8, upon reducing the volume of the pendant droplet, wrinkles were rapidly formed on the surface of the droplet. At a pH of 7.8, droplets formed by injecting the 0.224 g/L carboxylated fullerene aqueous solution into the toluene with 0.05 g/L PSP2VP3.5 did not coalesce, even when the droplets were forced into physical contact by forcing one droplet on the syringe into an existing droplet (Figure 2). This indicates that the formed interfacial film was elastic and very stable, which is consistent with the results presented by the Monteux group.[32] For calculation of the elastic and loss modulus of the interfacial film, interfacial dilatational rheology was performed using a pendant drop tensiometer coupled to an oscillating drop generator. As an example, Figure S4a shows the interfacial

DOI: 10.1021/acsami.7b07154
ACS Appl. Mater. Interfaces 2017, 9, 34389−34395

tension acquired during the droplet oscillation with frequency = 0.125 and deformation = 6%. As shown in Figure S4b,c, the elastic modulus was always much greater than the loss modulus in the entire frequency range used for the measurements, which confirms that the interfacial film is elastic. In contrast, at pH 11.17, although the interfacial tension is reduced by the addition of fullerene, wrinkling behavior was not observed when the volume of the droplet was reduced. Moreover, coalescence was observed when two droplets were forced into physical contact. At pH 4.84, the interfacial tension was technically not measurable, because of the formation of a solid film at the water/toluene interface, as was also observed by others.[33] Consequently, with variation of the pH, the strength of interactions between the fullerene and the copolymer can be tuned.

For a further demonstration that an elastic solid film was formed at a pH of 4.84, the volume in the pendant drop was increased, such that the reduction in the interfacial tension and gravitation forces extended the droplet to the point where a droplet would fall to the bottom of the measurement cell. However, as shown in Figure 3, and Video S1 in the Supporting Information, the droplet extended, forming a neck connecting the droplet (one reservoir) to the syringe (a second reservoir). With time, the neck stretched into a tubule, connecting the syringe to the droplet at the base of the chamber, such that the aqueous phase could be continuously pumped from the syringe into the droplet. This thin tubule of the aqueous phase in the toluene solution was stabilized by the formation of the elastic film at the interface. Plateau–Rayleigh instabilities and the breakup of the stream into droplets were suppressed, in a manner similar to that seen with the formation of nanoparticle surfactants.[34] In this example, the tubule was formed by injecting a 0.08 g/L fullerene solution (pH = 4.84), at a rate of 4 mL/min into 0.1 g/L PSP2VP12.5 toluene solution. Subsequent to the formation of the tubule, the aqueous phase was continuously passed through the tubule, causing the droplet at the base of the chamber to increase in volume with time. These results demonstrate that the interfacial film is not only elastic but also very stable and that there are strong interactions between the fullerene and the block polymer. The same phenomenon was not observed when the flow rate was less than 4 mL/min. However, at pH 7.8 and 11.17, since the aqueous phase was more basic, the degree of protonation of the P2VP decreased, and tubule formation was not observed, regardless of the injection speed. Consequently, pH provides a simple means of controlling the strength of the interaction between the functionalized fullerenes and the polymer.

The interfacial tension of homopolymer P2VP was also investigated in the presence of the functional fullerene. The equilibrium interfacial tension between pure water and 0.1 g/L P2VP in toluene was ~5.5 mN/m (Figure 4). When the 0.112 g/L fullerene (pH = 7.8) solution was used, the equilibrium interfacial tension decreased to ~4.5 mN/m, because of the interactions between the carboxylated fullerene and the P2VP. Upon comparison of the interfacial tension of 0.1 g/L PSP2VP3.5 and P2VP polymer in toluene with a 0.112 g/L fullerene (pH = 7.8) solution, the rate of reduction in the interfacial tension with PSP2VP3.5 was more rapid than that with P2VP. The time-dependent reduction in the interfacial tension was described by

$$\gamma(t) = \gamma_\infty + (\gamma_0 - \gamma_\infty)e^{(-t/\tau)} \quad (1)$$

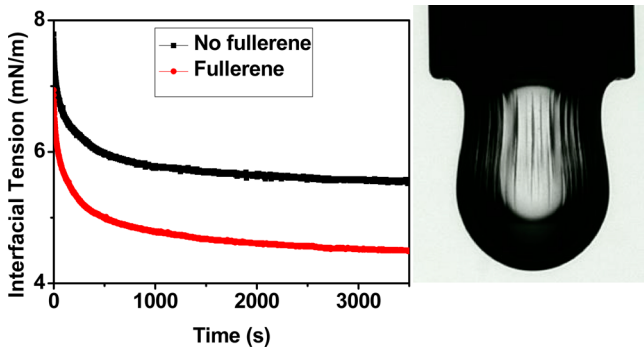

Figure 4. Time dependence of the interfacial tension for 0.1 g/L P2VP toluene solution with and without 0.112 g/L carboxylated fullerene aqueous solution (pH = 7.8). The imaging is the wrinkling film formed in the presence of fullerene.

where $\gamma(t)$, γ_0, and γ_∞ are the dynamic interfacial tension, the interfacial tension at time $t = 0$, and the equilibrium interfacial tension, respectively. τ is the characteristic relaxation time. τ for PSP2VP3.5 was found to be 408 s, while for P2VP, τ = 440 s indicating that the rate of interfacial assembly was controlled by the P2VP block and that the attached PS chain, although quite soluble in toluene, did not influence the interfacial adsorption. After the interfacial assembly of the homopolymer and block copolymer equilibrated, the aqueous phase was withdrawn from the droplet, decreasing the volume and the interfacial area of the droplet. At a volume reduction (remaining volume V/initial volume V_0) of 36% and 26.7%, corresponding to the interfacial area reduction (remaining area A/initial area A_0) of 46.7% and 43.2%, the interfacial assemblies of the PSP2VP3.5 copolymer and P2VP homopolymer were observed to wrinkle. Consequently, a much larger compression of the homopolymer layer is required to induce wrinkling than for the copolymer, indicating that the copolymer more effectively covers the interface. This is in agreement with the greater reduction in the interfacial tension for the block copolymer. The difference, more than likely, results from an enhanced localization of the block copolymer at the interface, since the P2VP block is covalently bound to the PS which is soluble in toluene only. This effectively anchors the P2VP block at the interface. For the homopolymer case, the homopolymer assembly with the fullerene can be forced into the aqueous phase, providing an alternate route for the homopolymer assembly to respond to the applied compression.

For further exploration into the effect of the functionalized fullerene on the interfacial assembly, dynamic interfacial tension experiments were performed using an amine-terminated polystyrene, $PSNH_2$, dissolved in toluene. With a 0.112 g/L fullerene solution (pH = 7.8; Figure 5), the interfacial tension was reduced because of the interactions of the amine terminus of the polymer with the carboxylic acid functional groups on the fullerene. With an increase of concentration of $PSNH_2$, the equilibrium interfacial tension was seen to decrease. This indicates that nanoparticle surfactants were formed at the interface between the water and toluene. At a pH of 7.8, as the volume of the pendant drop was decreased, the assembly wrinkled, but only if the assembly was aged for ~1 h. For a 0.5 g/L $PSNH_2$, wrinkling became evident at a V/V_0 of 15.9%, which is lower than that for 0.5 g/L PSP2VP3.5, where wrinkling was observed at a V/V_0 of 39.4%. Consequently, even though the reduction in the interfacial energy is substantial, a significant reduction in the interfacial area is required to induce

DOI: 10.1021/acsami.7b07154
ACS Appl. Mater. Interfaces 2017, 9, 34389–34395

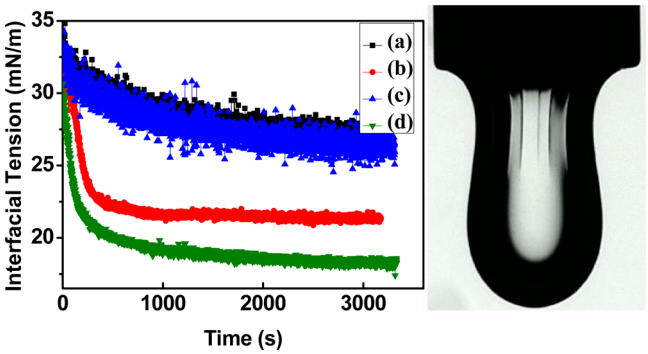

Figure 5. Time dependence of the interfacial tension for 0.112 g/L carboxylated fullerene aqueous solution (pH = 7.8) and (b) 0.5 g/L and (d) 1.0 g/L $PSNH_2$ in toluene; Control experiments in the absence of fullerene with (a) 0.5 g/L and (c) 1.0 g/L $PSNH_2$ in toluene. The image on the right is the wrinkling state of the fullerene with 0.5 g/L $PSNH_2$.

wrinkling. Unlike nanoparticle surfactants formed with larger inorganic nanoparticles, where wrinkling occurs at a much larger V/V_0, for the fullerene−$PSNH_2$ nanoparticle surfactants, the areal density of the assembly must be lower.

3.2. Dynamic Adsorption of Carboxylate Fullerene at the Interface. The different pH condition results in the entirely different adsorption kinetics of the fullerene to the interface. The interfacial tension as a function time for an aqueous dispersion of fullerene at different pH values in contact with a 0.05 g/L PSP2VP12.5 toluene solution is shown in Figure 6. The concentration of fullerene was 0.25, 0.224, and

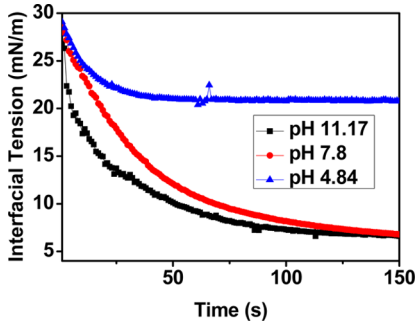

Figure 6. Dynamic interfacial tension of carboxylated fullerene with 0.05 g/L PSP2VP12.5 at different pH values.

0.08 g/L corresponding to a pH of 11.17, 7.8, and 4.84, respectively. It should be noted that the concentration used (0.224 and 0.08 g/L) is the maximum concentration of carboxylated fullerene in the resulted pH condition. The interfacial tension is seen to decrease rapidly initially (regardless of the pH). However, with increasing adsorption time, markedly different behavior is observed. At a pH of 4.84, the interfacial tension decreased to ∼20.9 mN/m, and then remained constant. At a pH of 7.8, the initial decrease in the interfacial tension is similar to that seen at a pH of 4.84. However, after ∼25 s, a very sharp decrease in the interfacial tension was seen, decreasing to values of less than 3 mN/m. At a pH of 11.17, the initial decrease in the interfacial tension is more rapid, and the interfacial tension continues to decrease to a value less than 3 mN/m. It should be noted that, for pH values of 4.84, an autowrinkling phenomenon was observed (see Video S3 in the Supporting Information), where the adsorbed layer on the interface, without a reduction in the volume of the droplet, spontaneously began to wrinkle. This behavior also precludes an accurate measurement of the interfacial tension, since it is evident that a film has been produced at the interface. One usually associates a wrinkling behavior with a compression of the assemblies at the interface where the areal density of the element on the interface is increased to the point where either elements must be ejected from the interface to accommodate the reduction in the interfacial area to avoid wrinkling, or the assembly is strong enough to remain intact as the assembly is forced out of a planar arrangement. Here, though, the adsorption rate is very rapid, and the molecular weight of the P2VP block is sufficiently high, so that a cross-linked network is rapidly formed that is swollen by both water and toluene. As more functionalized fullerenes interact with the P2VP, the cross-link density increases, causing a deswelling of the network which, in the plane of the interface, corresponds to a compressive force that give rise to the observed spontaneous wrinkling behavior.

AFM experiments were performed on a droplet that was transferred to a silicon substrate (Figure S5). Because of the geometry of the droplet, the transferred layer corresponds to a double layer, when the aqueous phase is removed from the droplet and the droplet collapses. We also cannot be absolutely certain that all of the residual, nonadsorbed fullerenes are removed, even though water was used to rinse the transferred droplet. The double layer that was transferred for 0.05 g/L PSP2VP12.5 in toluene without the fullerene in the aqueous phase was 10.0 ± 1.0 nm. If functionalized fullerene is present in the aqueous phase, the thickness of the double layer increases to 12.6 ± 1.0 nm, which is slightly thicker than that of pure polymers. Although AFM experiments exhibit some sample−sample variations, it could demonstrate that the interlayer at the toluene/water interface is a monolayer of polymers with some fullerene particles. Consequently, the picture that emerges is that the fullerene and the P2VP block interpenetrate (which would be expected if a cross-linked layer is formed) and that solvated polystyrene is tethered to the cross-linked layer, anchored by the P2VP block. From the AFM measurements it is difficult, if not impossible, to quantify the extent to which the polystyrene chains are stretched at the interface. Figure 7 illustrates the assembly of fullerenes and PSP2VP12.5 at the water/toluene interface.

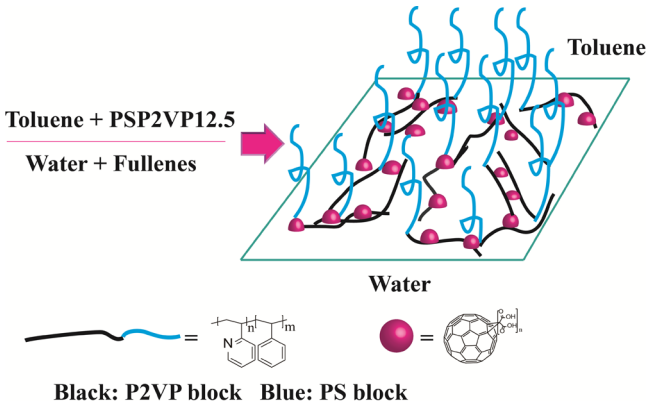

Figure 7. Schematic diagram of fullerene−PSP2VP compound assembly at the water/toluene interface, where the linear lines stand for PSP2VP biblock copolymers, and spheres represent carboxylated fullerene molecules.

DOI: 10.1021/acsami.7b07154
ACS Appl. Mater. Interfaces 2017, 9, 34389−34395

4. CONCLUSION

Using carboxylic-acid-functionalized fullerene in water and polymer PSP2VP, P2VP, and $PSNH_2$ in toluene, the self-assembly of fullerene at the oil/water interface was investigated. The dynamic interfacial tension data show that the interaction between fullerene and polymer or copolymer results in the formation of a cross-linked network at the interface. The layer that is formed at the interface is a robust, elastic layer that can support a compressive load and wrinkle. The assemblies are sensitive to pH, and at the appropriate pH and concentrations, Plateau−Rayleigh instabilities can be suppressed, enabling the stabilization of a jet of aqueous phase that was strong enough to act as a conduit of the aqueous phase through toluene. At low pH, a self-wrinkling behavior was observed, because of a rapid cross-linking of the adsorbed P2VP that the fullerene nanoparticles can enter into with the polymers and result in the reduction of interfacial tension. At different pH values, the interfacial interaction between the fullerenes with the polymers was different. At pH 7.8 and pH 4.84, a robust and jammed film was found at the water/toluene interface irrespective of the chemical structure of polymers. Interestingly, at pH 4.84, the interaction was very strong, and the adsorption of fullerene onto the interface was fast, which resulted in the *in situ* formation of the tube at the interface. The interaction between fullerene and the polymer attributes the hydrogen bonds.

■ ASSOCIATED CONTENT

Supporting Information

The Supporting Information is available free of charge on the ACS Publications website at DOI: 10.1021/acsami.7b07154.

Additional figures showing dynamic interfacial tension, interfacial dilatational rheology, AFM images, and a height profile of the film (PDF)

Video S1: formation of tubule by injecting at a rate of 4 mL/min into 0.1 g/L PSP2VP12.5 toluene solution (droplet disconnects and falls) (MPG)

Video S2: formation of tubule by injecting at a rate of 4 mL/min into 0.1 g/L PSP2VP12.5 toluene solution (droplet remains on syringe) (MPG)

Video S3: autowrinkling phenomenon for the droplet of 0.08 g/L fullerene solution (pH = 4.84) in 0.05 g/L PSP2VP12.5 toluene solution (MPG)

■ AUTHOR INFORMATION

Corresponding Author

*E-mail: russell@mail.pse.umass.edu.

ORCID

Rongqiang Li: 0000-0002-7427-8799

Anju Toor: 0000-0002-8613-7547

Thomas P. Russell: 0000-0001-6384-5826

Notes

The authors declare no competing financial interest.

■ ACKNOWLEDGMENTS

This work was supported by the U.S. Department of Energy, Office of Science, Office of Basic Energy Sciences, Materials Sciences and Engineering Division under Contract DE-AC02-05-CH11231 within the Adaptive Interfacial Assemblies Towards Structuring Liquids program (KCTR16). Portions of the work were carried out as a User Project at the Molecular Foundry, which is supported by the Office of Science, Office of Basic Energy Sciences, of the U.S. Department of Energy under Contract DE-AC02-05CH11231. We thank the China Scholarship Council for a State Scholarship Fund and Henan Advance Talent International Cultivation Fund to enable R.L. to do research in LBNL as a Visiting Scholar for 1 year.

■ REFERENCES

(1) Binks, B. P.; Tyowua, A. T. Oil-in-oil emulsions stabilised solely by solid particles. *Soft Matter* **2016**, *12* (3), 876−887.

(2) Böker, A.; He, J.; Emrick, T.; Russell, T. P. Self-assembly of nanoparticles at interfaces. *Soft Matter* **2007**, *3* (10), 1231−1248.

(3) Mendoza, A. J.; Guzman, E.; Martinez-Pedrero, F.; Ritacco, H.; Rubio, R. G.; Ortega, F.; Starov, V. M.; Miller, R. Particle laden fluid interfaces: dynamics and interfacial rheology. *Adv. Colloid Interface Sci.* **2014**, *206*, 303−319.

(4) Tavernier, I.; Wijaya, W.; Van der Meeren, P.; Dewettinck, K.; Patel, A. R. Food-grade particles for emulsion stabilization. *Trends Food Sci. Technol.* **2016**, *50*, 159−174.

(5) Tonga, G. Y.; Moyano, D. F.; Kim, C. S.; Rotello, V. M. Inorganic Nanoparticles for Therapeutic Delivery: Trials, Tribulations and Promise. *Curr. Opin. Colloid Interface Sci.* **2014**, *19* (2), 49−55.

(6) Garbin, V.; Crocker, J. C.; Stebe, K. J. Nanoparticles at fluid interfaces: exploiting capping ligands to control adsorption, stability and dynamics. *J. Colloid Interface Sci.* **2012**, *387* (1), 1−11.

(7) Grzelczak, M.; Vermant, J.; Furst, E. M.; Liz-Marzán, L. M. Directed self-assembly of nanoparticles. *ACS Nano* **2010**, *4* (7), 3591−3605.

(8) Booth, S. G.; Dryfe, R. A. Assembly of nanoscale objects at the liquid/liquid interface. *J. Phys. Chem. C* **2015**, *119* (41), 23295−23309.

(9) Zanini, M.; Isa, L. Particle contact angles at fluid interfaces: pushing the boundary beyond hard uniform spherical colloids. *J. Phys.: Condens. Matter* **2016**, *28*, 313002.

(10) Hua, X.; Bevan, M. A.; Frechette, J. Reversible Partitioning of Nanoparticles at an Oil−Water Interface. *Langmuir* **2016**, *32* (44), 11341−11352.

(11) Ding, T.; Rudrum, A. W.; Herrmann, L. O.; Turek, V.; Baumberg, J. J. Polymer-assisted self-assembly of gold nanoparticle monolayers and their dynamical switching. *Nanoscale* **2016**, *8* (35), 15864−15869.

(12) Bai, R. X.; Xue, L. H.; Dou, R. K.; Meng, S. X.; Xie, C. Y.; Zhang, Q.; Guo, T.; Meng, T. Light-Triggered Release from Pickering Emulsions Stabilized by TiO2 Nanoparticles with Tailored Wettability. *Langmuir* **2016**, *32* (36), 9254−9264.

(13) Maestro, A.; Guzmán, E.; Ortega, F.; Rubio, R. G. Contact angle of micro- and nanoparticles at fluid interfaces. *Curr. Opin. Colloid Interface Sci.* **2014**, *19* (4), 355−367.

(14) Lin, Y.; Skaff, H.; Emrick, T.; Dinsmore, A.; Russell, T. P. Nanoparticle assembly and transport at liquid-liquid interfaces. *Science* **2003**, *299* (5604), 226−229.

(15) Lin, Y.; Böker, A.; Skaff, H.; Cookson, D.; Dinsmore, A.; Emrick, T.; Russell, T. P. Nanoparticle assembly at fluid interfaces: structure and dynamics. *Langmuir* **2005**, *21* (1), 191−194.

(16) He, J.; Zhang, Q.; Gupta, S.; Emrick, T.; Russell, T. P.; Thiyagarajan, P. Drying droplets: a window into the behavior of nanorods at interfaces. *Small* **2007**, *3* (7), 1214−1217.

(17) He, J.; Niu, Z.; Tangirala, R.; Wang, J.-Y.; Wei, X.; Kaur, G.; Wang, Q.; Jutz, G. n.; Böker, A.; Lee, B.; et al. Self-assembly of tobacco mosaic virus at oil/water interfaces. *Langmuir* **2009**, *25* (9), 4979−4987.

(18) Briggs, N. M.; Weston, J. S.; Li, B.; Venkataramani, D.; Aichele, C. P.; Harwell, J. H.; Crossley, S. P. Multiwalled Carbon Nanotubes at the Interface of Pickering Emulsions. *Langmuir* **2015**, *31* (48), 13077−13084.

(19) Feng, T.; Hoagland, D. A.; Russell, T. P. Assembly of acid-functionalized single-walled carbon nanotubes at oil/water interfaces. *Langmuir* **2014**, *30* (4), 1072−1079.

(20) Wan, W.; Zhao, Z.; Hughes, T. C.; Qian, B.; Peng, S.; Hao, X.; Qiu, J. Graphene oxide liquid crystal Pickering emulsions and their assemblies. *Carbon* **2015**, *85*, 16−23.
(21) Sun, Z.; Feng, T.; Russell, T. P. Assembly of graphene oxide at water/oil interfaces: tessellated nanotiles. *Langmuir* **2013**, *29* (44), 13407−13413.
(22) Shao, J. J.; Lv, W.; Yang, Q. H. Self-assembly of graphene oxide at interfaces. *Adv. Mater.* **2014**, *26* (32), 5586−5612.
(23) Chen, L.; Huang, L.; Zhu, J. Stitching graphene oxide sheets into a membrane at a liquid/liquid interface. *Chem. Commun. (Cambridge, U. K.)* **2014**, *50* (100), 15944−15947.
(24) Babu, S. S.; Mohwald, H.; Nakanishi, T. Recent progress in morphology control of supramolecular fullerene assemblies and its applications. *Chem. Soc. Rev.* **2010**, *39* (11), 4021−4035.
(25) Nakashima, N.; Ishii, T.; Shirakusa, M.; Nakanishi, T.; Murakami, H.; Sagara, T. Molecular Bilayer-Based Superstructures of a Fullerene-Carrying Ammonium Amphiphile: Structure and Electrochemistry. *Chem. - Eur. J.* **2001**, *7* (8), 1766−1772.
(26) Wakai, H.; Momoi, T.; Shinno, T.; Yamaudhi, T.; Tsubokawa, N. A novel polymer-grafted C60 fullerene having both hydrophilic and hydrophobic chains. *Mater. Chem. Phys.* **2009**, *118* (1), 142−147.
(27) Matsumoto, M.; Tachibana, H.; Azumi, R.; Tanaka, M.; Nakamura, T.; Yunome, G.; Abe, M.; Yamago, S.; Nakamura, E. Langmuir-Blodgett Film of Amphiphilic C60 Carboxylic Acid. *Langmuir* **1995**, *11* (2), 660−665.
(28) Shrestha, L. K.; Hill, J. P.; Tsuruoka, T.; Miyazawa, K.; Ariga, K. Surfactant-assisted assembly of fullerene (C60) nanorods and nanotubes formed at a liquid-liquid interface. *Langmuir* **2013**, *29* (24), 7195−7202.
(29) Shrestha, L. K.; Shrestha, R. G.; Hill, J. P.; Tsuruoka, T.; Ji, Q.; Nishimura, T.; Ariga, K. Surfactant-Triggered Nanoarchitectonics of Fullerene C60 Crystals at a Liquid-Liquid Interface. *Langmuir* **2016**, *32* (47), 12511−12519.
(30) Fujita, N.; Yamashita, T.; Asai, M.; Shinkai, S. Formation of [60]fullerene nanoclusters with controlled size and morphology through the aid of supramolecular rod-coil diblock copolymers. *Angew. Chem., Int. Ed.* **2005**, *44* (8), 1257−1261.
(31) Marinova, K.; Alargova, R.; Denkov, N.; Velev, O.; Petsev, D.; Ivanov, I.; Borwankar, R. Charging of oil− water interfaces due to spontaneous adsorption of hydroxyl ions. *Langmuir* **1996**, *12* (8), 2045−2051.
(32) Le Tirilly, S.; Tregouët, C.; Bône, S. p.; Geffroy, C. d.; Fuller, G.; Pantoustier, N. g.; Perrin, P.; Monteux, C. c. Interplay of hydrogen bonding and hydrophobic interactions to control the mechanical properties of polymer multilayers at the oil−water interface. *ACS Macro Lett.* **2015**, *4* (1), 25−29.
(33) Knoche, S.; Vella, D.; Aumaitre, E.; Degen, P.; Rehage, H.; Cicuta, P.; Kierfeld, J. Elastometry of deflated capsules: elastic moduli from shape and wrinkle analysis. *Langmuir* **2013**, *29* (40), 12463−12471.
(34) Toor, A.; Helms, B. A.; Russell, T. P. Effect of Nanoparticle Surfactants on the Break-Up of Free-Falling Water Jets During Continuous Processing of Reconfigurable Structured Liquid Droplets. *Nano Lett.* **2017**, *17* (5), 3119−3125.

DOI: 10.1021/acsami.7b07154
ACS Appl. Mater. Interfaces 2017, 9, 34389−34395